Clay Minerals, (2016) **51**, 435–444

Biodegradable polymer nanocomposites based on natural nanotubes: effect of magnetically modified halloysite on the behaviour of polycaprolactone

VIERA KHUNOVÁ[1,*], IVO ŠAFAŘÍK[2], MARTIN ŠKRÁTEK[3], IVAN KELNAR[4] AND KATARÍNA TOMANOVÁ[1]

[1] *Institute of Natural and Synthetic Polymers, Slovak University of Technology, FCHPT, Radlinského 9, Bratislava 812 37, Slovakia*

[2] *Department of Nanobiotechnology, Biology Centre, CAS, Na Sádkách 7, České Budejovice 370 05, Czech Republic*

[3] *Institute of Measurement Science, Slovak Academy of Sciences, Dúbravská cesta 9, Bratislava 841 04, Slovakia*

[4] *Institute of Macromolecular Chemistry, Academy of Science of the Czech Republic, Heyrovsky Sq. 2, Prague 16206, Czech Republic*

(*Received 17 November 2015; revised 14 February 2016; Guest Editor: Pooria Pasbakhsh*)

ABSTRACT: The present study explores the effect of a magnetically modified halloysite (mHNT) surface on the structure and properties of biodegradable polymer nanocomposites based on poly ε-caprolactone (PCL). Halloysite nanotubes (HNTs) have been modified by a scalable and tunable procedure using magnetic Fe oxide particles prepared by microwave-assisted synthesis from ferrous sulfate at high pH. The HNT content in composites prepared in melt varied from 5 to 30 wt.%. Application of magnetically modified HNT to PCL resulted in the formation of soft magnetic materials. Analyses of the nanocomposite structure revealed that both natural and magnetized HNTs, as well as free magnetite particles are dispersed uniformly in the polymer matrix. Investigation of the mechanical and physical properties confirmed that the reinforcing ability of HNTs was not affected by magnetic modification.

KEYWORDS: magnetically modified HNTs, biodegradable polymer nanocomposites, polycaprolactone.

The effort devoted in recent decades to the development of polymer nanocomposites has resulted in increased exploitation in industries such as automotive and packaging, and in medicine. At present the most widespread polymer nanocomposites are based on platy layered silicates, mainly montmorillonite. In spite of a number of advantages important for polymer nanocomposites, HNTs, until recently, did not attract much attention from the scientific community. Due to less abundant surface hydroxyl groups, HNT, in contrast to montmorillonite, is readily dispersed in polymers without the need for exfoliation (Lvov *et al.*, 2014). Furthermore, halloysite can adopt (depending on the crystallization conditions and geological occurrences) a variety of morphologies: from spheroidal and platy to tubular particle shapes (Joussein *et al.*, 2005). The most common morphology is tubular. Due to a large aspect ratio (the length of the nanotubes is in the range 0.2–1.5 μm, whereas the inner and outer diameters of the tubes are 10–30 and 40–70 nm, respectively), the application of tubular HNTs in polymers leads to a significant reinforcing effect (Lee & Chang, 2013; Pasbakhsh *et al.*, 2013). A further advantage is that modification of HNTs is much easier and simpler than with the other natural layered silicates or synthetic nanofillers. Significant enhancement of HNT-based polymer

*E-mail: viera.khunova@stuba.sk
DOI: 10.1180/claymin.2016.051.3.05

nanocomposite properties has been achieved by silanization (*e.g.* Murariu *et al.*, 2012) and even without any HNT treatment (Lee & Chang, 2013).

For potential biomedical application it is very important that, unlike platy silicates, HNTs can be used as a low-cost nanoscale container for encapsulation of a broad variety of substances including drugs, enzymes and DNA (Ghebaur *et al.*, 2012; Liu *et al.*, 2014; Lvov *et al.*, 2014). A further important property required for application in medicine is that HNT exhibits a high level of biocompatibility (Verma *et al.*, 2012) and is not toxic for cells (Vergaro *et al.*, 2010). From the point of view of biomedical applications, HNTs are very efficient fillers for nanocomposites based on a biopolymer matrix, *e.g.* alginate (Chiew *et al.*, 2014), polylactide (Liu *et al.*, 2013a), pectin (Cavallaro *et al.*, 2013) and chitosan (Liu *et al.*, 2013b).

Polymers in general are a typical example of electrically resistant and non-magnetic materials. For numerous applications, however, conductive and/or magnetic properties together with other special properties of polymers are required. Similarly to conductive polymers, magnetic polymers can be prepared by synthesis or by incorporation of magnetic fillers into thermoplastic polymers (Carosio *et al.*, 2010) or elastomers (Kruželák *et al.*, 2012, 2014). Due to the spherical shape, the reinforcing effect of magnetic fillers, especially with high filler content, is very limited and/or absent. A further drawback of nanoscale magnetic fillers is that they usually agglomerate in the polymer matrix. The importance of magnetic polymer nanocomposites in environmental and biomedical applications was highlighted by Kalia *et al.* (2014).

The HNTs are diamagnetic materials. For potential biomedical application it is very important that HNTs can be converted into their magnetically responsive derivatives. There are several techniques that can be used for magnetic modification of diamagnetic materials. In most cases the magnetization of HNT is based on the attachment of magnetic Fe oxide nano- or microparticles to the surface or within the pores of the treated materials; many of them require technologically complex processes, however (Safarik *et al.*, 2012).

In light of the above-mentioned potential of HNTs, the role of magnetized HNTs in the properties and structure of PCL were considered in the present study.

EXPERIMENTAL

Materials

The poly ε-caprolactone (PCL) (CAPA 6800, PCL, $Mw = 80{,}000$ g mol^{-1}, melting point = 60°C, melt flow index (MFI) = 2.4 g/10 min (2.16 kg, 160°C)), was obtained from Perstorp (Sweden). The HNT was received from Imerys Tableware (Auckland, New Zealand). Ferrous sulfate and NaOH were obtained from Sigma Aldrich in the Czech Republic.

Magnetization of HNT

The preparation of magnetized HNT (mHNT) was based on the use of magnetic Fe oxide nano- and microparticles prepared by a microwave-assisted process from ferrous sulfate at pH 12. For the following experiments, 10 g of HNT was mixed with 120 mL of a magnetic Fe oxide particles suspension (the volume ratio between solid material and water was 1:4). The mixing time was at least 3 min to enable complete mixing. Then the mHNT was dried completely at 60°C (Safarik & Safarikova, 2014).

Composite preparation

The composites were prepared from PCL and native or magnetized HNT *via* melt mixing in a Brabender W50-EH chamber at 140°C using a rotor speed of 60 rpm. Dog bone-shaped specimens (a gauge length of 40 mm, EN ISO 527-2:2012, Sample size 5B) were prepared in a laboratory micro-injection moulding machine (DSM). The barrel and mould temperatures were 135 and 130°C, respectively.

Magnetic-properties measurements

The magnetic properties of the samples studied were measured using a Quantum Design MPMS XL-7 SQUID magnetometer. Magnetization as a function of temperature was measured in the temperature range of 1.8–300 K. The sample of magnetized HNT (mHNT) was cooled from room temperature to the lowest temperature in the zero applied field and the magnetization was measured after application of the field (8000 Am^{-1}), while warming (ZFC, zero-field-cooled measurement). For field-cooled (FC) measurements, the sample was cooled in the presence of a field and magnetization was measured as a function of temperature while cooling. Measurement of the magnetization as a function of field was made at room temperature (298 K) up to a field of 7 T.

Mechanical testing

Tensile tests were carried out using an Instron 5800 apparatus at 22°C and crosshead speed of 50 mm/min.

https://doi.org/10.1180/claymin.2016.051.3.05 Published online by Cambridge University Press

Dynamic mechanical thermal analysis (DMA) was performed in single-cantilever mode using a DMA DX04 T apparatus at 1 Hz and a heating rate of 1°C/min from −120 to 100°C.

Characterization of structure

The scanning electron microscopy (SEM) studies of the samples were performed using a JEOL JSM-7500F instrument (Japan). The HNT samples were prepared by its application on conductive carbon adhesive tape. PCL/HNT samples were prepared by breaking after cooling. The fracture surfaces were sputtered with a gold layer using a Sputter Coater BALZERS SCD 050 coating machine.

For transmission electron microscope (TEM) (Tecnai) observations, ultrathin (60 nm) sections were prepared under liquid nitrogen using an Ultracut UCT (Leica) ultra-microtome.

The phase composition was studied by powder X-ray diffraction (XRD) using the Philips PW 1050 diffractometer (Cu-*K*α radiation).

RESULTS AND DISCUSSION

Magnetic properties

The structures of HNT (Fig. 1a) and magnetite (Fig. 1b) were investigated first. The SEM images show clearly that most of the HNT particles have a tubular shape within the range of aspect ratio from 5 to 12. HNT particles with a small (1–2) aspect ratio are also present.

Preparation of magnetic-labelled magnetite nanoparticles and their μm-sized aggregates was performed in standard kitchen microwave oven (700 W, 2450 MHz). The formation of magnetite nanoparticles can be summarized as follows:

$$Fe^{2+} + 2\,OH^- \rightarrow Fe(OH)_2$$

$$3Fe(OH)_2 + 1/2O_2 \rightarrow Fe_3O_4 + 3H_2O$$

The post-magnetization procedure employed prepared magnetic Fe oxide particles (Fig. 1b) which were mixed with the HNTs to be modified and dried completely. The stable magnetically responsive HNTs

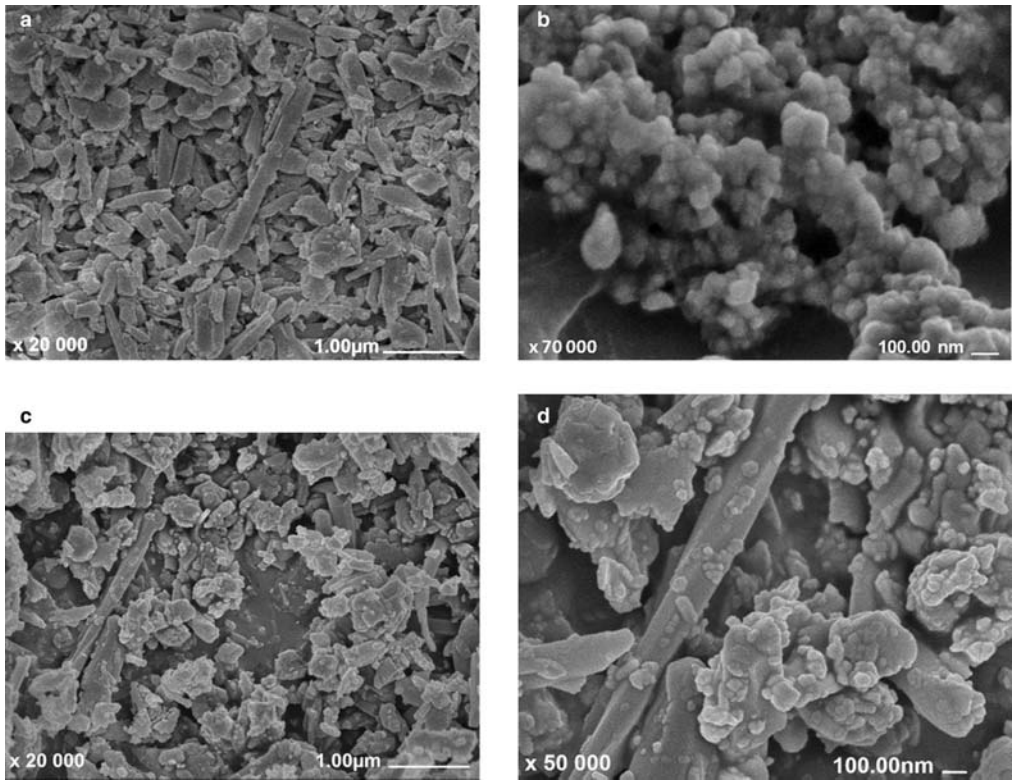

FIG. 1. SEM images of: (a) untreated HNTs, (b) magnetic nanoparticles used for modification, (c,d) magnetized HNTs (mHNTs).

https://doi.org/10.1180/claymin.2016.051.3.05 Published online by Cambridge University Press

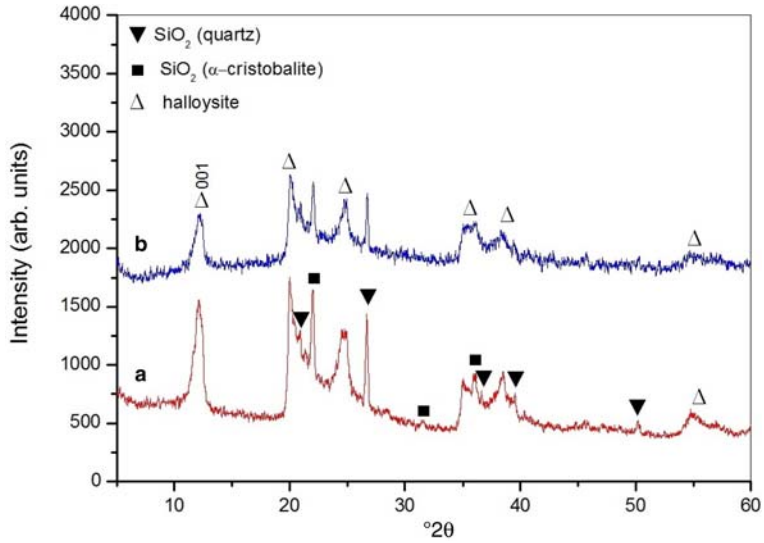

FIG. 2. XRD patterns of (a) untreated HNTs, (b) magnetized HNTs (mHNTs). (Δ): halloysite, (▼): SiO_2 quartz, (■): SiO_2 α-cristobalite.

(mHNTs) had been prepared. The 18.3 wt.% of magnetic Fe oxide particles in mHNTs (Fig. 1c,d) was determined from the known volume of magnetic Fe oxide particles suspension added to the known amount of halloysite. In a parallel measurement, the dry weight of Fe oxide particles was determined. Based on experience with several dozen magnetically modified materials, all magnetic particles adhere firmly to the modified material under the experimental conditions used.

As shown in Fig. 1b, microwave-assisted synthesis led to the formation of magnetic Fe oxide nanoparticles with diameters ranging between 30 and 100 nm. During the synthesis, the nanoparticles formed stable

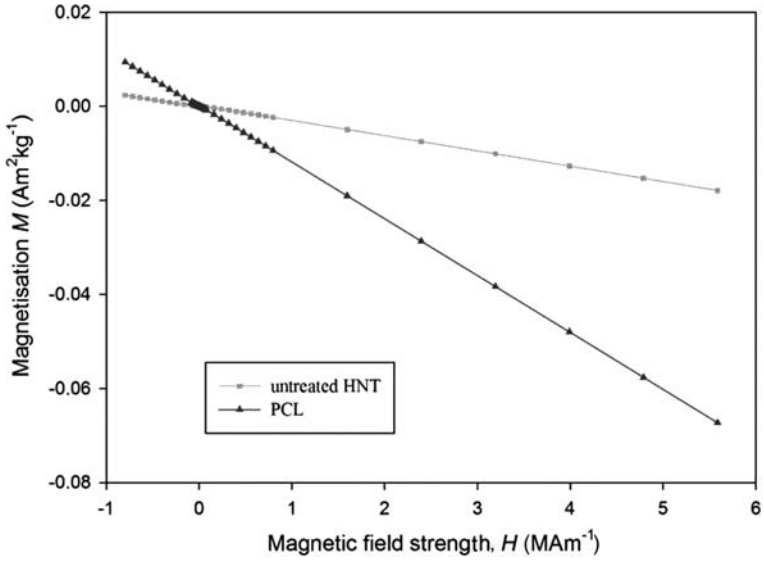

FIG. 3. Hysteresis loops of PCL and untreated HNTs.

https://doi.org/10.1180/claymin.2016.051.3.05 Published online by Cambridge University Press

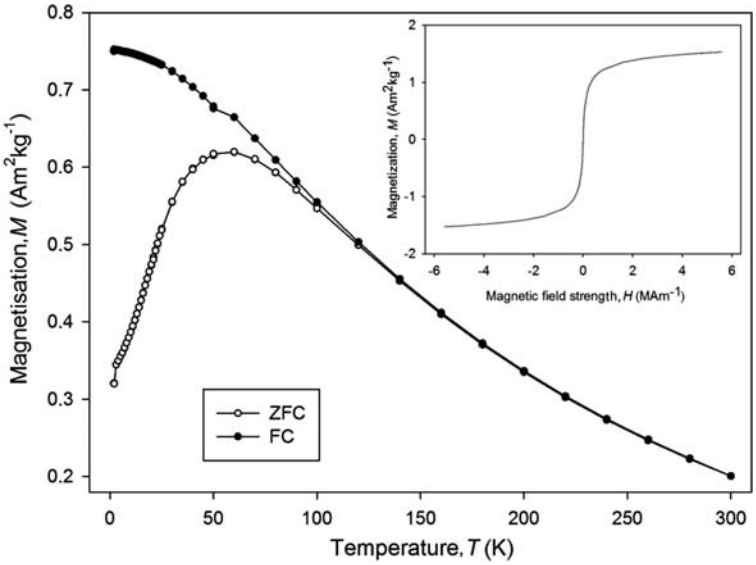

FIG. 4. ZFC/FC curve of mHNTs. Inset shows a hysteresis loop recorded at room temperature.

μm-sized agglomerates and thus an intercalation of Fe oxide particles within the lumen of HNTs was not possible. From Fig. 1c,d it is evident that Fe oxide particles are located on HNT external surfaces and as 'free' individual particles and/or agglomerates in samples of mHNT. Thus, mHNT was formed by both magnetized HNT as well as free Fe oxide particles.

The XRD pattern of an untreated halloysite sample is shown in Fig. 2a. The sample contains a typical 001 diffraction at 12.07°2θ ($d = 7.33$ Å), which is ascribed to halloysite ($Al_2(OH)_4Si_2O_5 \cdot 2H_2O$) (Wang *et al.*, 2013). However, the characteristic diffraction peaks of quartz (SiO2) and α-cristobalite (SiO_2) are always present to a large extent. In the case of

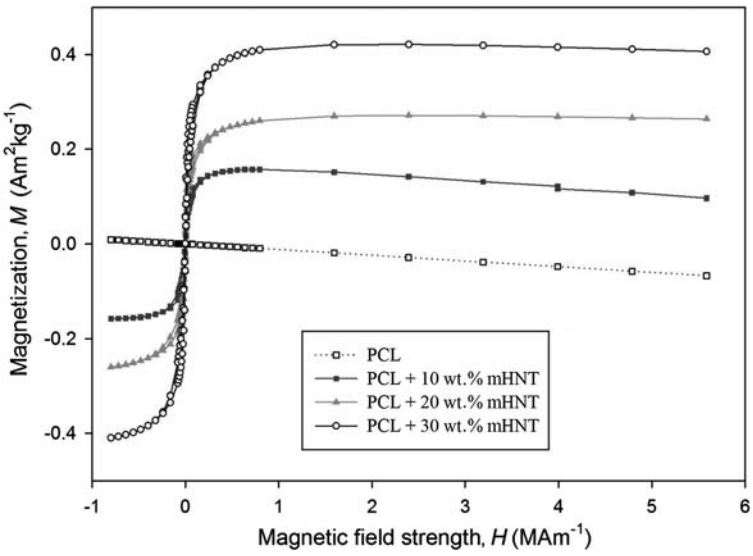

FIG. 5. Hysteresis loops for the PCL and PCL + mHNT nanocomposites recorded at room temperature.

https://doi.org/10.1180/claymin.2016.051.3.05 Published online by Cambridge University Press

TABLE 1. Magnetic properties of the PCL + mHNT composites prepared.

Sample name	Coercivity, H_C (A/m)	Saturation magnetization M_S (mAm^2/kg)	Remanence M_R (mAm^2/kg)
PCL + 10 wt.% mHNT	4535	96	21
PCL + 20 wt.% mHNT	3262	263	27
PCL + 30 wt.% mHNT	4774	406	57

mixtures of halloysite–magnetic particles, (Fig. 2b), the characteristic diffraction patterns for crystalline magnetite are clearly absent. Nevertheless, because Cu-$K\alpha$ radiation was used in the diffraction experiment, the typical strong fluorescence which increases the background in the diffraction pattern for Fe-oxide species is presented in the pattern. As a result, the diffraction intensity of all crystalline phases was reduced substantially.

Hysteresis loops for the PCL and untreated HNT show clearly the diamagnetic character of the polymer matrix and untreated HNTs (Fig. 3). The ZFC/FC measurement of the mHNT sample (Fig. 4) shows the irreversibility of the curves and the blocking temperature (T_B) of 60 K (defined as the maximum of the $M(T)$ curve in the ZFC conditions); this behaviour and the hysteresis loop (inset in Fig. 4) confirm that magnetized HNT belongs to the group of superparamagnetic materials.

Hysteresis loops (Fig. 5) of prepared magnetic PCL + mHNT composites confirm that addition of 10–30 wt.% mHNT into PCL resulted in the formation of soft magnetic materials with significantly less saturation magnetization compared to mHNT. The saturation magnetization (M_S) of the PCL + 30 wt.% mHNT magnetic composite is 0.406 Am^2 kg^{-1} and negligible remanence (M_R) and coercivity (H_C) were observed in the hysteresis loop (Table 1).

Mechanical properties and morphology

From a comparison of PCL/HNT and PCL/mHNT composites in the concentration range of 5–30 wt.%

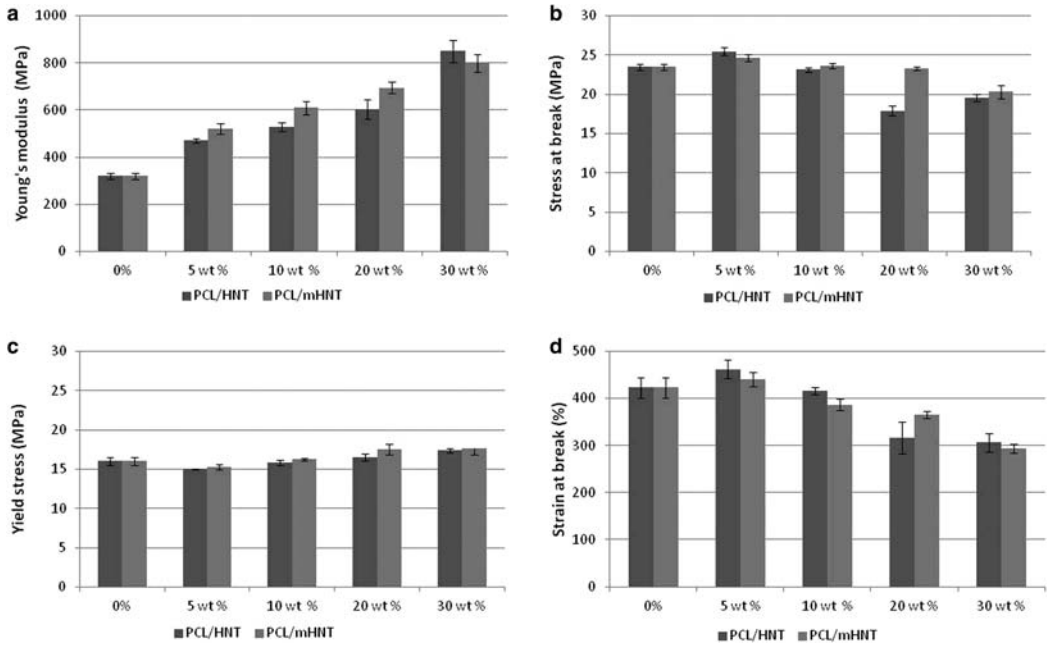

FIG. 6. Effect of untreated HNTs and mHNTs on mechanical properties of PCL: (a) Young's modulus, (b) stress at break, (c) yield stress, and (d) strain at break.

https://doi.org/10.1180/claymin.2016.051.3.05 Published online by Cambridge University Press

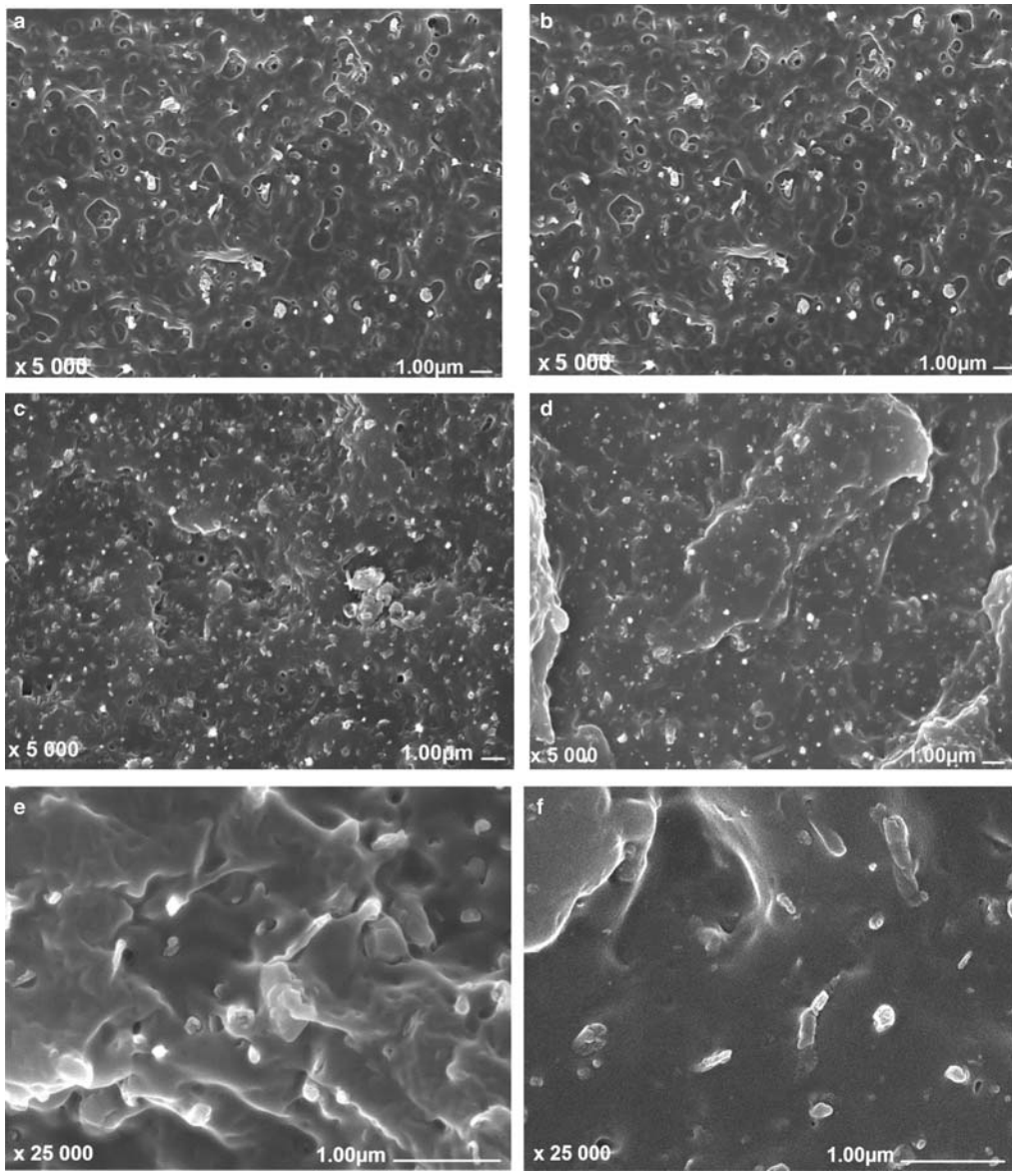

FIG. 7. SEM images of cryo-fractured surfaces of PCL/HNT nanocomposites: (a) PCL/10 wt.% HNTs; (b) PCL/10 wt.% mHNTs; (c) 30 wt.% HNTs; (d) PCL/30 wt.% mHNTs; (e) 30 wt.% HNTs; and (f) PCL/30 wt.% mHNTs.

studied, it is evident that the most important mechanical parameters *e.g.* yield stress, stiffness and elongation at break are practically unaffected by HNT magnetization, or even improved (Fig. 6). If compared with pure PCL as well as PCL/HNT composites, improvement of Young's modulus (Fig. 6a) and stress at break (Fig. 6b) in PCL/mHNT composites is even greater. An analogous effect, although not as significant, was observed in the case of yield stress (Fig. 6c).

Taking into account the presence of additional spherical particles of Fe oxide at the expense of magnetized HNTs (Fig. 1c,d), the mechanical properties are much better than would otherwise be expected. The explanation for this is highlighted by comprehensive SEM and TEM analyses.

https://doi.org/10.1180/claymin.2016.051.3.05 Published online by Cambridge University Press

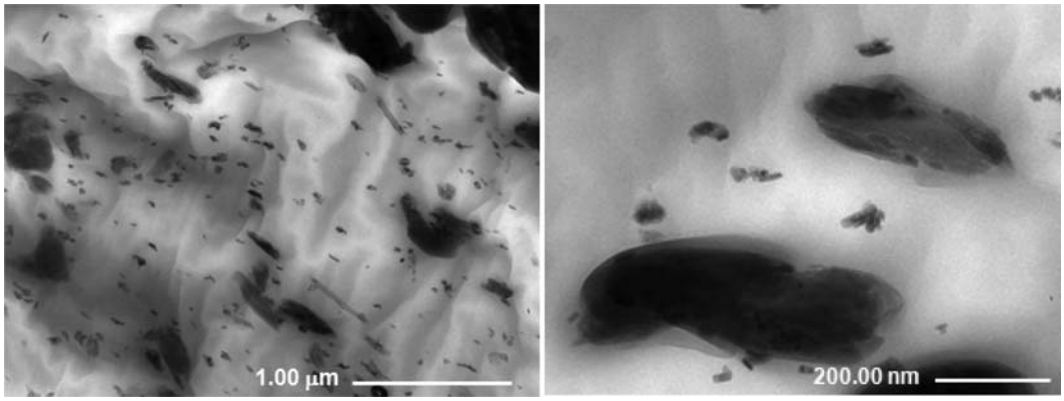

FIG. 8. TEM images of PCL/20 wt.% mHNT nanocomposites.

Although individual filler particles are well dispersed in the polymer matrix in composites based on untreated HNTs (Fig. 7a,c,e), particle size seems to be greater if compared with corresponding composites containing magnetized HNTs (Fig. 7b,d,f). In view of better mechanical properties of nanocomposites containing magnetized HNT, this result is apparently caused by the presence of both well dispersed magnetized HNT as well as single Fe oxide particles in the PCL matrix (Fig. 8). As shown in Fig. 2, characteristic diffraction peaks for Fe-oxide phases were not found.

Rheology of PCL/HNT composites

Rheological results indicate practically the same course of complex viscosity/frequency dependence of PCL/HNT and PCL/mHNT composites in Fig. 9, which corresponds to a similar structure of reinforcement (Fig. 7a,b). There is an obvious absence of significant interactions between particles indicated by a similar course of viscosity/frequency dependence for composites based on natural and modified HNTs and PCL at a low shear rate. The more significant decrease in viscosity at higher frequency (shear rate) corresponds to the presence of tubular HNTs. The fact that rheological behaviour of composites based on modified HNTs is similar to the analogous system with an unmodified HNT indicates that magnetic modification does not affect the processing of composites.

Dynamic mechanical analysis

The temperature dependence of loss modulus (Fig. 10) indicates a more marked intensity of the peak

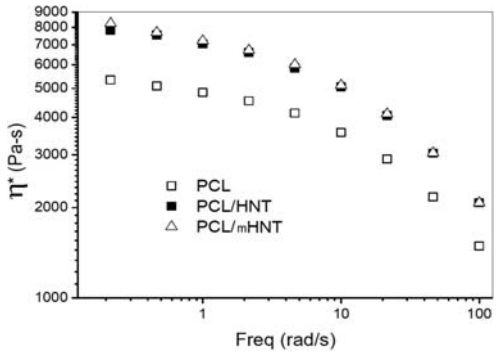

FIG. 9. Effect of HNTs and mHNTs on complex viscosity, η*, of PCL at 140°C. The HNT and mHNT content in PCL was 20 wt.%.

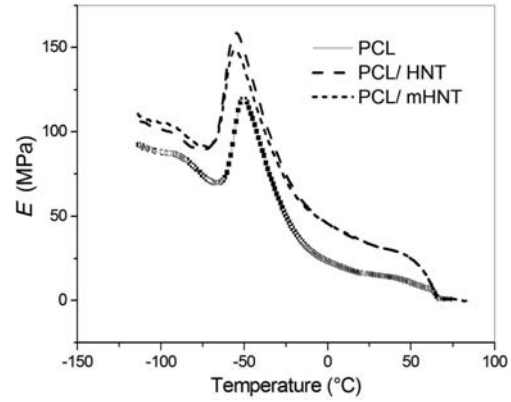

FIG. 10. Temperature dependence of loss modulus E'' of PCL/20 wt.% HNTs and PCL/20 wt.% mHNTs.

https://doi.org/10.1180/claymin.2016.051.3.05 Published online by Cambridge University Press

representing the glass transition temperature (T_g) of PCL composites in comparison with pure PCL. This is due to PCL-HNT interactions affecting the mobility of PCL chains to a slightly less significant extent for mHNT, probably due to different surface parameters. The shift of T_g to lower temperatures corresponds to greater chain mobility due to increased free volume in the case of anisotropic nanofillers with lengths exceeding the typical gyration radii of polymer chains (Cai *et al.*, 2015).

CONCLUSIONS

Magnetically modified HNTs were prepared using a simple, scalable and tunable procedure. By application of magnetized HNT in PCL, soft magnetic biocompatible polymer nanocomposites have been prepared. Apart from magnetic properties, a positive effect of HNT magnetization was observed on the structure and mechanical properties of composites. The fact that the rheological behaviour of composites based on magnetized HNT is similar to the analogous system with unmodified HNT indicates that modification does not affect processing of composites.

The combination of PCL and magnetic HNT allows us to create new, advanced, environmentally friendly, biocompatible and biodegradable soft magnetic polymer nanocomposites suitable for diverse biomedical applications.

ACKNOWLEDGEMENT

The authors appreciate the financial support provided by the Slovak Research and Development Agency (N°. APW-14-0175), the Slovak Grant Agency VEGA (Grant 1/0361/14 and 2/0152/13) and by the Czech Science Foundation (Grants 13-15255S and 13-13709S). The authors also thank Imerys Tableware New Zealand Ltd. for the supply of halloysite.

REFERENCES

Cai N., Dai Q., Wang Z., Luo X., Xue Y. & Yu F. (2015) Toughening of electrospun poly(L-lactic acid) nanofiber scaffolds with unidirectionally aligned halloysite nanotubes. *Journal of Materials Science*, **50**, 1435–1445.

Carosio F., Fina A. & Coisson M. (2010) Polypropylene-based ferromagnetic composites. *Polymer Bulletin*, **65**, 681–689.

Cavallaro G., Lazzara G. & Milioto S. (2013) Sustainable nanocomposites based on halloysite nanotubes and pectin/polyethylene glycol blend. *Polymer Degradation and Stability*, **98**, 2529–2536.

Chiew S.C.C., Poh P.E., Pasbakhsh P., Tey B.T., Yeoh H. K. & Chan E.S. (2014) Physicochemical characterization of halloysite/alginate bionanocomposite hydrogel. *Applied Clay Science*, **101**, 444–454.

Ghebaur A., Garea S.A. & Iovu H. (2012) New polymer-halloysite hybrid materials-potential controlled drug release system. *International Journal of Pharmaceutics*, **436**, 568–573.

Joussein E., Petit S., Churchman J., Theng B., Righi D. & Delvaux B. (2005) Halloysite clay minerals – a review. *Clay Minerals*, **40**, 383–426.

Kalia S., Kango S., Kumar A., Haldorai Y., Kumari B. & Kumar R. (2014) Magnetic polymer nanocomposites for environmental and biomedical applications. *Colloid and Polymer Science*, **292**, 2025–2052.

Kruželák J., Hudec I. & Dosoudil R. (2012) Elastomeric magnetic composites – physical properties and network structure. *Polimery*, **57**, 25–32.

Kruželák J., Sýkora R., Dosoudil R. & Hudec I. (2014) Magnetic composites based on natural rubber prepared by using peroxide and sulphur curing system. *Polymer Advanced Technologies*, **25**, 995–1000.

Lee K.-S. & Chang Y.-W. (2013) Thermal, mechanical, and rheological properties of poly(ε-caprolactone)/halloysite nanotube nanocomposites. *Journal of Applied Polymer Science*, **128**, 2807–2816.

Liu M., Zhang Y. & Zhou C.H. (2013a) Nanocomposites of halloysite and polylactide. *Applied Clay Science*, **75**, 52–59.

Liu M., Wu Ch., Jiao Y., Xiong S. & Zhou C.H. (2013b) Chitosan-halloysite nanotubes nanocomposite scaffolds for tissue engineering. *Journal of Materials Chemistry B*, **1**, 2078–2089.

Liu M., Jia Z., Jia D. & Zhou C.H. (2014) Recent advance in research on halloysite nanotubes – polymer nanocomposite. *Progress in Polymer Science*, **39**, 1498–1525.

Lvov Y., Aerov A. & Fakhrullin R. (2014) Clay nanotube encapsulation for functional biocomposites. *Advances in Colloid and Interface Science*, **207**, 189–198.

Murariu M., Dechie A., Paint Y., Peeterbroeck S., Bonnaud L. & Dubois P. (2012) Polylactide (PLA)-halloysite nanocomposites: production, morphology and key-properties. *Journal of Polymers & the Environment*, **20**, 932–943.

Pasbakhsh P., Churchman G.J. & Keeling J.L. (2013) Characterisation of properties of various halloysites relevant to their use as nanotubes and microfibre fillers. *Applied Clay Science*, **74**, 47–57.

Safarik I. & Safarikova M. (2014) One-step magnetic modification of non-magnetic solid materials. *International Journal of Materials Research*, **105**, 104–107.

Safarik I., Horska K., Pospiskova K. & Safarikova M. (2012) Magnetically responsive activated carbons for bio- and environmental applications. *International Review of Chemical Engineering*, **4**, 346–352.

https://doi.org/10.1180/claymin.2016.051.3.05 Published online by Cambridge University Press

Vergaro V., Abdullayev E., Lvov Y., Zeitoun A., Cingolani R., Rinaldi R. & Leporatti S. (2010) Cytocompatibility and uptake of halloysite clay nanotubes. *Biomacromolecules*, **11**, 820–82.

Verma K., Moore E., Blau W., Volkov Y. & Babu P.R. (2012) Cytotoxicity evaluation of nanoclays in human epithelial cell line A549 using high content screening and real-time impedance analysis. *Journal of Nanoparticle Research*, **14**, 1137.

Wang Q., Zhang J. & Wang A. (2013) Alkali activation of halloysite for adsorption and release of ofloxacin. *Applied Surface Science* **287**, 54–61.

https://doi.org/10.1180/claymin.2016.051.3.05 Published online by Cambridge University Press